

SUPPLEMENTARY INFORMATION

Evidence of Different Growth Regimes Coexisting within Biomimetic Layer-by-Layer Films

*Khalil Abdelkebir, Fabien Gaudière, Sandrine Morin-Grognet, Gérard Coquerel, Béatrice Labat, Hassan Atmani and Guy Ladam**

Laboratoire de Biophysique et Biomatériaux (La2B), SMS EA 3233, IMR FED 4114, Université de Rouen, Centre Universitaire d'Evreux, 1 rue du 7^{ème} Chasseurs, BP 281, 27002 Evreux Cedex, France. *E-mail: guy.ladam@univ-rouen.fr

Appendix A1. Assessment of the OWLS probing extent in thickness.

This appendix is aimed at checking the order of magnitude of the penetration depth of the OWLS probing wave, by computing its characteristic decay length Δz , according to the relation:^{S1,S2}

$$\Delta z = \frac{1}{\frac{2\pi}{\lambda} \sqrt{|N^2 - n^2|} \left[(N/n_F)^2 + (N/n)^2 - 1 \right]^\rho} \quad (1)$$

where $\lambda = 632.8$ nm is the wavelength of the probing laser beam, $N = N_{\text{TE}}$ or N_{TM} , $\rho = 0$ and 1 for the TE and TM mode respectively, and n and n_F are the respective refractive indices of the waveguide layer and the adlayer. With the values $N_{\text{TE}} = 1.607$, $N_{\text{TM}} = 1.573$, $n_F = 1.77915$ and $n = 1.425$ relative to the representative film described in Fig. 2A in the article, Eq. 1 provides the values $\Delta z_{\text{TE}} = 136$ nm and $\Delta z_{\text{TM}} = 151$ nm, which are close to the 150-200 nm range commonly cited in the literature.^{S3-S5}

Appendix A2. Proportionality relationship between the ATR-FTIR absorbance and the dry mass and thickness of ChS/PLL films.

This appendix is aimed at showing that the ATR-FTIR absorbance of the ChS/PLL films studied is proportional, in first approximation, to their dry mass and thickness. According to Harrick, the absorbance A corresponding to an IR peak is given by:^{S6}

$$A = A_0 \cdot \left(1 - e^{-\frac{2d}{d_p}} \right) \quad (2)$$

with A_0 the absorbance of an infinitely thick film, d the film thickness, and d_p the penetration depth of the probing evanescent wave in the adjacent environment. d_p , defined as the characteristic decay length of the wave intensity from the surface, is expressed by:

$$d_p = \frac{\lambda}{2\pi n_1 \sqrt{\sin^2 \theta - (n/n_1)^2}} \quad (3)$$

where λ is the wavelength of the incident wave, $n_1 = 2.42$ and n are the respective refractive indices of the ZnSe substrate and the film, and $\theta = 45^\circ$ is the angle of reflection. Using the value $n = 1.425$ obtained by OWLS (Fig. 2B in the article), and $\lambda = 10 \mu\text{m}$ ($\nu = 1/\lambda = 1000 \text{ cm}^{-1}$), the penetration depth of the incident beam within ChS/PLL films is $d_p = 1.69 \mu\text{m}$, which is very large compared to the film thickness. Under this condition, it is assumed that the Beer-Lambert law applies,^{S7} such that A is proportional to the mass of adsorbed polymers. A first order approximation of Eq. 3 also indicates that A is proportional to the film thickness, according to:

$$A \sim \frac{2 \cdot A_0}{d_p} \cdot d \quad (4)$$

Figure S1. Evolution of the optical thickness, as considered after each ChS/PLL layer pair (from OWLS data reported in Fig. 2C in the article). The line represents the linear regression fit and is accompanied by the corresponding determination coefficient $R^2 = 0.996$.

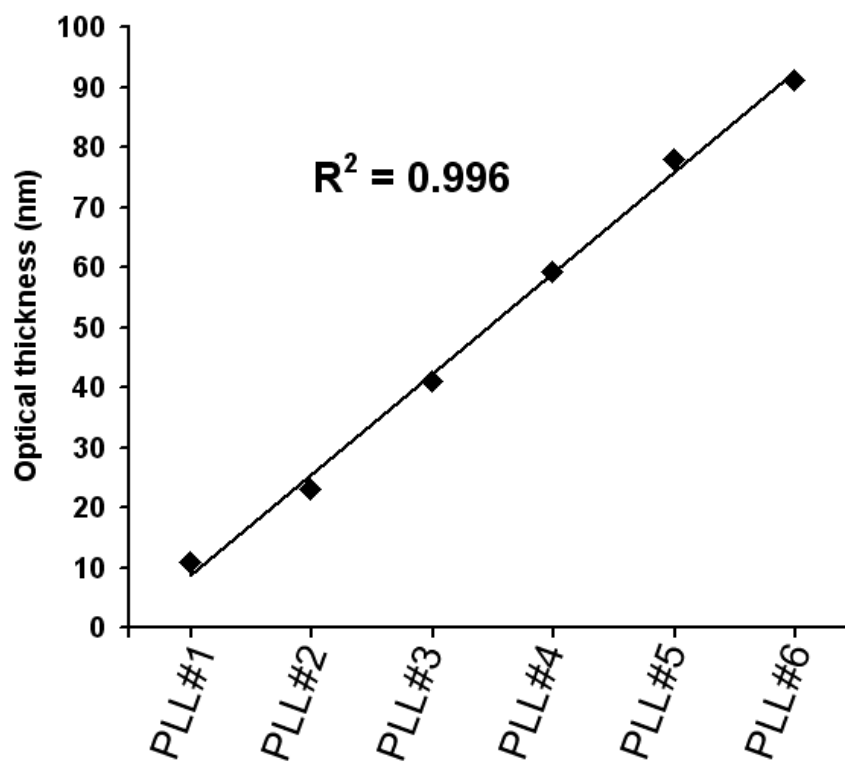


Figure S2. Typical 3D and 2D AFM images representing the topographies of (A) a PEI/(ChS/PLL)₆ film and (B) a PEI/(ChS/PLL)₆/ChS film built up onto glass substrates and analyzed in contact with the buffer solution. Mean roughness values R_a over three separate images ($20 \times 20 \mu\text{m}^2$) are accompanied by standard errors.

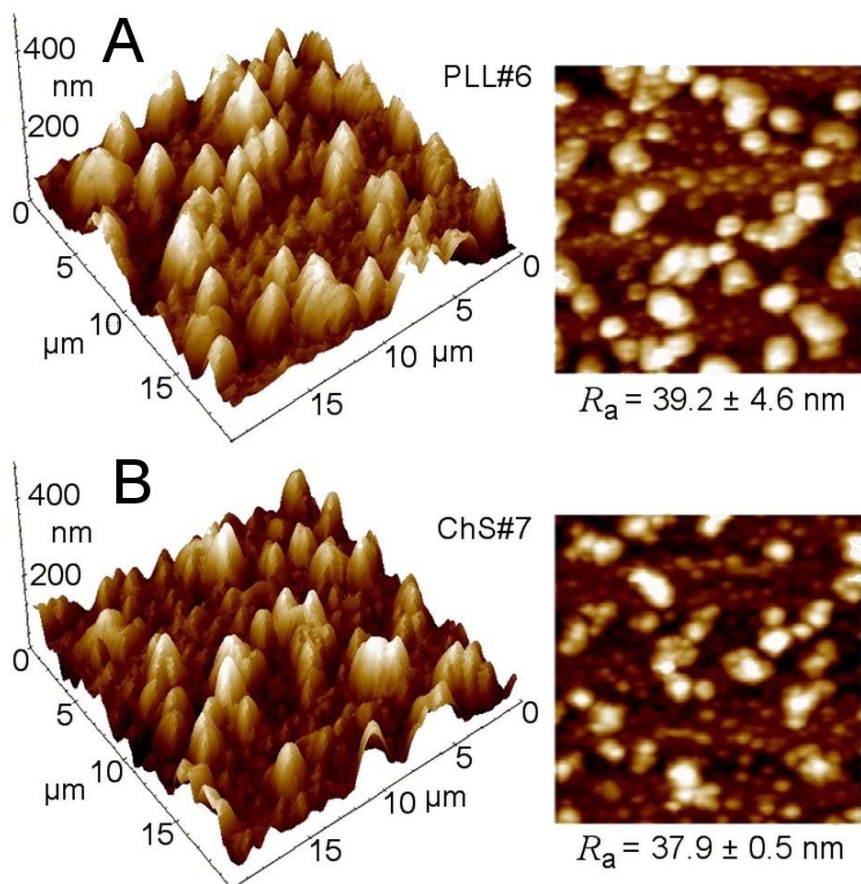


Figure S3. Optical micrograph of a dry PEI/(ChS/PLL)₆ film built up atop a QCM-D sensor. The surface was scratched with a needle, then dried, prior to observation. Continuity of the scratch boundary shows the continuity of the deposit.

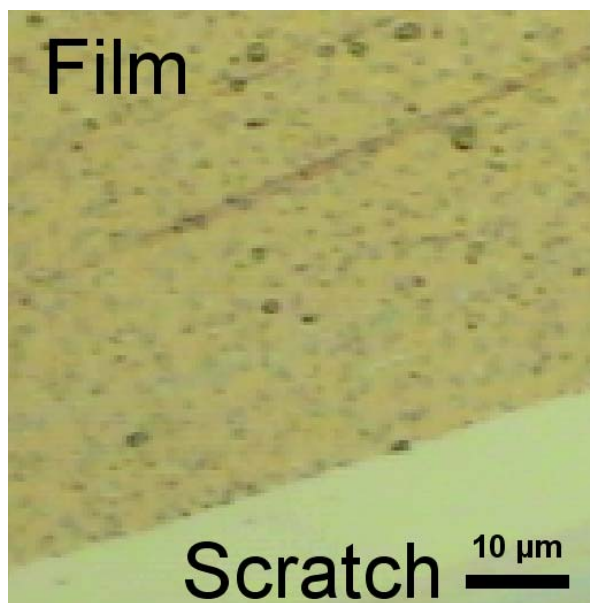
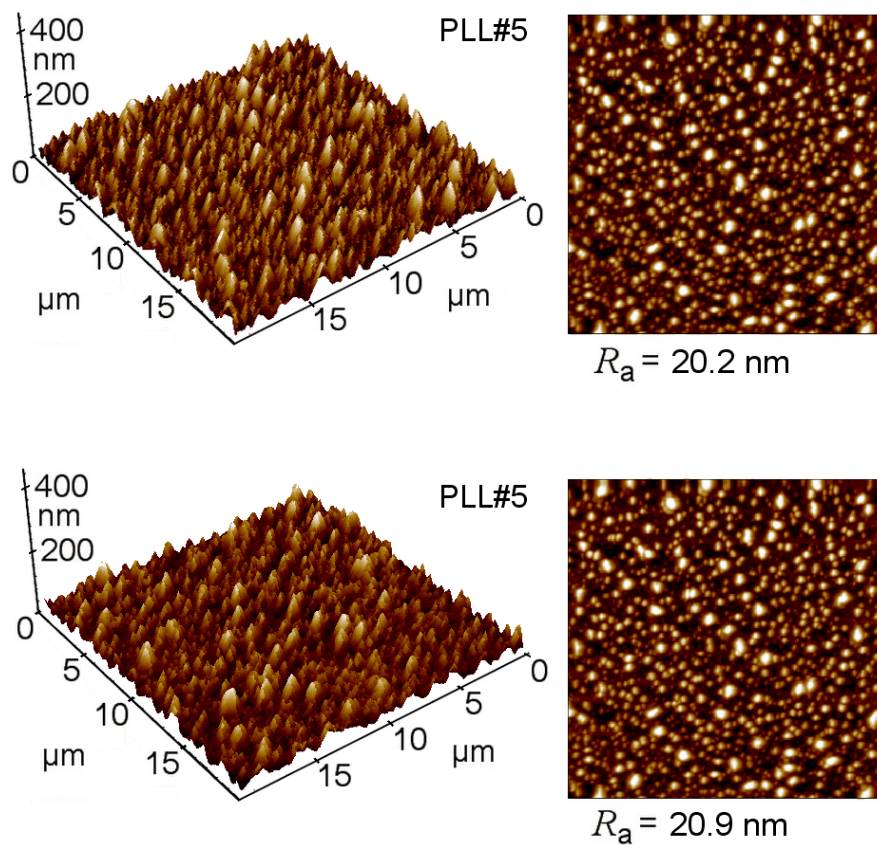


Figure S4. 3D and 2D AFM images representing the topography of a PEI/(ChS/PLL)₅ film built up onto a glass substrate and analyzed in contact with the buffer solution. Roughness values R_a were determined upon the total image area ($20 \times 20 \mu\text{m}^2$).



Références

- S1 C. Picart, C. Gergely, Y. Arntz, J. C. Voegel, P. Schaaf, F. J. G. Cuisinier and B. Senger, *Biosens. Bioelec.*, **2004**, *20*, 553.
- S2 K. Tiefenthaler and W. Lukosz, *J. Opt. Soc. Am. B*, **1989**, *6*, 209.
- S3 A. Tezcaner, D. Hicks, F. Bouldemais, J. Sahel, P. Schaaf, J. C. Voegel and P. Lavalley, *Biomacromolecules*, **2006**, *7*, 86.
- S4 F. Boulmedais, V. Ball, P. Schwinté, B. Frisch, P. Schaaf and J. C. Voegel, *Langmuir*, **2003**, *19*, 440.
- S5 C. Picart, P. Lavalley, P. Hubert, F. J. G. Cuisinier, G. Decher, P. Schaaf and J. C. Voegel, *Langmuir*, **2001**, *17*, 7414.
- S6 N. J. Harrick, *Internal Reflection Spectroscopy*, John Wiley & Sons Inc., New York, 1967.
- S7 A. Krzeminski, M. Marudova, J. Moffat, T. R. Noel, R. Parker, N. Wellner and S. G. Ring, *S. G.*, *Biomacromolecules*, **2006**, *7*, 498.